

Thermal Expansion Measurements on Coating Materials by Digital Image Correlation

R. J. Thompson and K. J. Hemker

Department of Mechanical Engineering
Johns Hopkins University, Baltimore, MD 21218, USA

ABSTRACT

Accurate knowledge of the thermal expansion behavior of thin structures is crucial to improving the performance of many modern thermomechanical systems. A completely contact free, image-based, highly adaptable technique for measuring displacement, strain, and the coefficient of thermal expansion of thin specimens from room temperature to approximately 1100 °C is presented and discussed. Fullfield digital image correlation is employed to extract the thermal expansion information as it is relatively simple, inexpensive, and provides many analysis points so statistics can be applied to fully and carefully examine the sample's deformation as a function of temperature. Thermal expansion results from a well-characterized Rene N5 superalloy are used to validate the experimental and data processing methodologies. The coefficient of thermal expansion for a 150 μm thick NiCoCrAlY bond coat layer found in contemporary thermal barrier coatings is presented and discussed as well. For the superalloy, the coefficient of thermal expansion increased monotonically from approximately 12 ppm/°C at room temperature to nearly 16 ppm/°C at 1050 °C. The NiCoCrAlY bond coat also exhibited monotonically increasing thermal expansion behavior but to a considerably greater extent, ranging from about 12.5 ppm/°C at room temperature to nearly 18 ppm/°C at 1050 °C.

INTRODUCTION

As mechanical devices move toward higher operating temperatures and smaller size scales, a secure understanding of the coefficient of thermal expansion (CTE) for each component of the apparatus is essential. Thermal barrier coatings (TBCs) for example, commonly used in modern gas turbines and jet engines, are dynamic, multi-layered structures consisting of a superalloy substrate, an intermetallic bond coat, a thermally grown oxide (TGO), and a ceramic top coat. These novel systems represent a classical application in which knowledge of the thermal expansion performance of each layer, and thus the CTE mismatch between the layers, is vital to quantifying the degradation and ultimate failure modes of the coating [1]. Recent TBC models [1-3], along with many other commercial engineering software applications, rely on the user to input reliable temperature-dependent thermal expansion information given most frequently by the true coefficient of linear (unidirectional) thermal expansion, as defined in Equation 1.

$$\alpha(T) = \frac{1}{L} \left(\frac{dL}{dT} \right)_p \quad (1)$$

For clarity, it should be noted that the CTE identified by Equation 1 is a material property because it describes expansion at every temperature in the analysis range; the reference temperatures, i.e. the start and end points of the experiment, do not need to be known. Another metric of CTE, the instantaneous (secant) coefficient of thermal expansion, can be used to describe variations in length associated with discrete, specific changes in temperature and is also sometimes used in science and engineering applications [4, 5]. Nevertheless, the instantaneous coefficient of thermal expansion is not a material property and all CTE values presented in this paper will pertain to the true coefficient of linear thermal expansion.

In practice, thermal expansion measurements are most commonly completed using a mechanical, rod-based dilatometer. These machines [4, 5] typically quantify CTE by determining the combined expansion of both the sample and a long push rod, and all displacements are registered outside of the heated zone. This technique is fairly simple, reliable, and possesses high temperature capability (generally > 1000 °C) but it is not, however, sufficient for materials which are extremely fragile and consequently incapable of actuating the comparatively heavy rod needed to measure CTE. Actual TBC bond coat layers, normally formed by a plasma spray or aluminizing procedure to the order of 50 - 100 μm thick [1], are therefore clearly not a candidate for standard mechanical dilatometry. Thus, as a result of the desire to assess the thermal expansion of a bond coat specimen that is most representative of what would be found in an actual TBC system, a noncontact method is required.

Optical experiments provide an attractive alternative to standard push rod dilatometry when it is necessary to evaluate the thermal expansion behavior of a completely free standing thin material [4, 5]. Dilatometers of this type can use a twin telescope comparator with a deflecting prism to gauge the change in distance between fiducial markers placed on the material of interest [6]. Another option involves simply measuring the position of the edges of a specimen using a laser-based system [7] or with regular incoherent light [8, 9]. Nonetheless, these techniques frequently necessitate that one dimension of the sample be considerably long, on the order of many millimeters usually, to acquire adequate resolution. Moreover, creating and applying sufficient fiducial markers on such a long yet thin (100 μm or less) free standing specimen constitutes a major challenge in and of itself. Laser-based interferometric dilatometers [10-12], which function on the principle of following the motion of interference fringes from two or more laser beams, are another viable choice when obtaining high temperature, high resolution thermal expansion data is desired. The setbacks associated with these systems include high costs due to the use of lasers, lenses, filters, detectors, pyrometers, and vacuum chambers, which in turn leads to considerable overall complexity. Furthermore, interferometric dilatometers require an initially reflective sample that must remain reflective throughout the test.

Digital image correlation (DIC), first applied to an experimental mechanics problem at the University of South Carolina [13], is another valuable optical technique which can extract displacement and strain fields that can possibly be nonlinear with relative ease from images taken during deformation in a contact free, direct manner. This is in stark contrast to each of the aforementioned references, which are only capable of overall, effective strain measurements on specimens that are assumed to be uniform in composition and thermal expansion behavior. DIC relies on the maximization of a cross correlation coefficient C_{xy} , determined by examining pixel intensity array subsets on two or more corresponding digital images (Equation 2). When done correctly, this maximization essentially “follows” selected regions centered at (x_i, y_i) on the sample surface and accordingly outputs the material description of motion for the given deformation.

$$C_{xy} = \frac{\sum I_0(x, y) \cdot I(x, y)}{\sqrt{\sum I_0^2(x, y) \cdot \sum I^2(x, y)}} \quad (2)$$

From this material description of motion, other mechanical variables such as displacement, strain, and CTE can be computed without major difficulties [14]. A significant amount of work devoted to

improving the efficiency and accuracy of the algorithms used for correlation is available [15-18] and the development of smarter, faster correlation routines continues to this day. As a result of this technical progress, numerous applications of DIC in both science and engineering continue to be discovered due to both the ease of capturing and the wealth of useful information that can be extracted simply from a set of digital images.

Considerably less research, however, is available regarding DIC setups for elevated temperature measurements. One investigation [19] utilizes fullfield DIC to quantify changes in the structure of different ceramic materials, using loss-of-correlation-time for given temperatures up to 500 °C as the metric, while others [20] illustrate the development of a mechanical and thermal expansion testing setup for experiments up to 650 °C. More recently, discrete (not fullfield) applications of DIC include systems designed to be easily adaptable to commercial tensile testing machines with reported temperature capability to 1200 °C [21] and 1600 °C [22]. A paper detailing the use of DIC to follow discrete markers located at the cold end of a quartz dilatometer up to 950 °C [23] is also available in the literature. In these reports, some noncontacting thermal strain data is presented [20-22] to approximately 650 °C, 1050 °C, and 1250 °C respectively, yet no attempts are made to calculate the corresponding temperature-dependent thermal expansion coefficient. Further, here, as with all of the previously mentioned dilatometry references, essentially no studies are accessible that account for the added complications of attaining thermal expansion values for very thin plasma sprayed or aluminized layers, which are more representative of the geometries, microstructures, and behavior of bond coats found in modern TBCs.

Thus, this paper seeks to outline a robust, uncomplicated, direct procedure that can be used to determine the thermal displacement, thermal strain, and CTE for entirely free standing materials with thicknesses on the order of 100 μm or less using a fullfield DIC scheme to temperatures of nearly 1100 °C, a combination for which significant discussion and data is currently unavailable in the literature.

MATERIALS AND PROCESSING

This section discusses the preparation of a Rene N5 superalloy and a 150 μm thick NiCoCrAlY bond coat alloy for thermal expansion testing. For the Rene N5 specimen, received from GE in the form of a 25.4 mm diameter uncoated button, wire EDM machining is applied to make a sample with a length, width, and thickness of approximately 25 mm x 5 mm x 5 mm, respectively. The NiCoCrAlY bond coat, processed by powder pressing at Pratt and Whitney in the shape of a bulk block, is created using the wire EDM and mechanical polishing to yield a specimen with a length of nearly 15 mm, a width of close to 5 mm, and a thickness of 150 μm . A final step before testing involves using a piece of 20 μm diamond paper to produce a subtle scratch pattern on the surfaces of each sample; this provides more than enough speckle contrast for subsequent image correlation analysis.

EXPERIMENTAL SETUP AND PROCEDURE

The major components of the image-based thermal expansion testing setup, illustrated in Figure 1, include: a small furnace with an optical viewport, a temperature controller, a high intensity metal halide light source, a three axis stage, a high resolution 6.6 Megapixel digital camera with variable long-working-distance optics, and a custom built computer for image capturing and analysis.

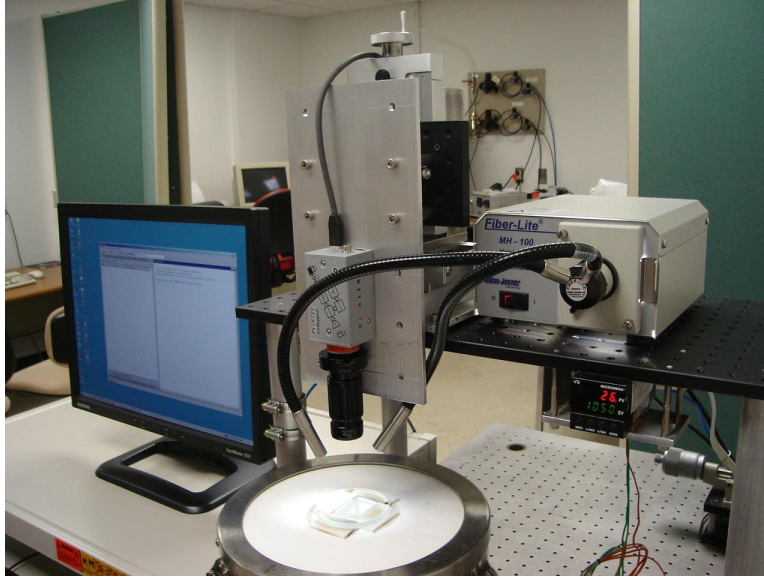


Figure 1. The image-based thermal expansion setup.

The modern equipment used in the construction of this test system enables significant improvement of the attainable peak temperature with respect to previous attempts of a similar nature [20] due to the ability of the high intensity white light illumination to overpower the infrared (IR) radiation emanating from the heating coils of the furnace. This, in addition to the camera's on-chip low IR sensitivity, allows for sufficient contrast to be captured on specimens heated to temperatures of nearly 1100 °C. Moreover, the high 3000 x 2208 resolution of the color digital camera allows very precise images with a bit depth of 24 to be captured; this too simply could not be obtained with the technology available just a few years in the past.

Currently, the limiting factor in defining the peak operating temperature of the setup is attributed to the maximum power of 750 Watts that the furnace can draw when the temperature controller is effectively eliminated from the circuit. Adjustment of the position of the insulation located under the window (Figure 1) to create a smaller effective viewing area will limit heat loss through the viewport and accordingly increase the peak operating temperature, yet the exposed area must still be kept large enough such that the image signal is not blocked and can reach the camera sufficiently. After some experimentation, setting the exposed viewport area to 20 mm x 30 mm proved to be a good compromise permitting testing up to roughly 1100 °C while still allowing for images from samples 25 mm in length to fully register on the camera's CCD chip.

Two aspects of the test system that are difficult to see in Figure 1 include a temperature probe located at the vertical centerline of the furnace and coplanar with the specimen, all inside the heated zone, as well as a small tube that directs laboratory air over the top surface of the furnace window to encourage satisfactory mixing of the heated gases in the optical path. Without this provision, significant, seemingly random distortions occur and any resulting images must be discarded.

Thus, by using the experimental components discussed above, both strain and temperature can be quantified in a completely noncontact manner. No wires need to be attached to the sample for things such as Ohmic heating and thermocouple temperature measurement. This is favorable because application of these electric lines can be extremely cumbersome on fragile sub 100 μm thin materials; these wires can also introduce significant rigid body translation during heating and cooling, which can cause the sample to move off the optical axis and possibly out of the field of view of the camera. Unnecessary large motions of the specimen and subsequent adjustments of the position of the optics to follow the sample lowers both the accuracy and resolution of the DIC

results. Creep complications due to mechanical gripping of the specimen, together with variable surface emissivity calibration issues associated with temperature measurement by pyrometry, are also avoided.

The procedure for conducting the DIC-based thermal expansion test is not difficult. First, a newly prepared and polished specimen is loaded into the furnace and heated once to 1000 °C and then slowly cooled back to room temperature to eliminate any thermal-related instabilities that may exist on the sample's surface. Furthermore, for the alloys tested in this study, this one simple step forms an exceptionally stable oxide on the imaging surface and provides more than enough speckle contrast for the image correlation routine; no further surface decoration is necessary. Once this initial thermal cycle is completed, the focus, lighting, and field of view are adjusted to the levels shown in Figure 2 and a room temperature image is captured.

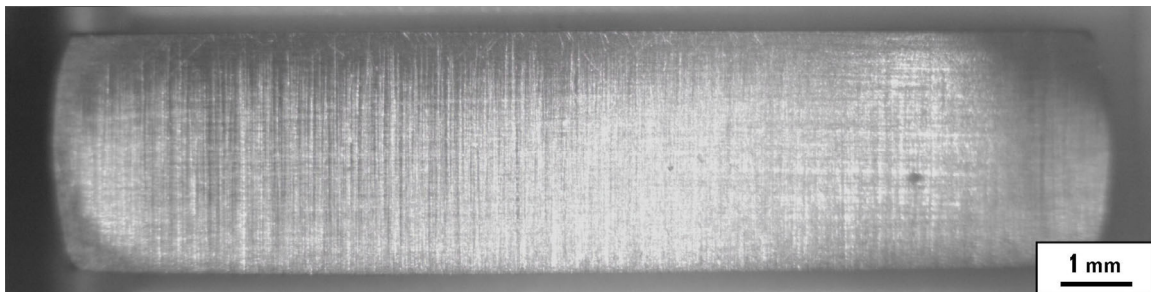


Figure 2. Room temperature image of the Rene N5 sample.

In order to not waste hard disk space, captured images are cropped before saving; the dimensions of the image in Figure 2 are 3000 x 720, which corresponds to a file size of 6.3 MB. Here, the current optical zoom settings yield a coverage ratio of approximately 100 pixels/mm; this resolution requires an effective working distance, i.e. the distance between the sample surface and the first lens in the optics, of nearly 150 mm. After the room temperature image is recorded, the temperature is increased, usually by increments of 50 °C, and the sample is soaked at the new setting for 15 minutes or until the variation in the reading is +/- 1 °C or less. This ensures that thermal equilibrium is reached and the temperature value is accurate. Once these conditions are met, another image is captured. This procedure is repeated until the desired peak temperature is reached, normally around 1050 °C to 1100 °C. The final step involves post processing the captured images with an automatic, user-friendly Matlab™ program developed at Johns Hopkins University to calculate displacement, strain, and CTE of the specimen, all as a function of temperature.

Close attention must be paid to a number of important imaging parameters in order for this type of experiment to work properly. Setting the illumination intensity to its maximum value and using a low camera exposure time (20 milliseconds) makes certain that the IR radiation can be overpowered throughout the selected temperature range. In addition to this, although global changes in image brightness generally do not degrade the correlation results, local changes in intensity and loss of focus must be avoided during the test. Finally, on-camera frame averaging is employed to reduce the slight amount of noise associated with CCD sensors. Typically, each image is averaged over 50 frames (exposures); in total, performing this task and then saving the image to the computer's hard disk takes about 5 seconds.

DIGITAL IMAGE CORRELATION ANALYSIS

The computational methods applied for this paper are derived from an automated, user-interface-orientated suite of software written in Matlab™ at the Johns Hopkins University. The first release of this popular tool is available online [24] and a recent paper [25] illustrates an application of the code to tension testing of extremely small, translucent samples. For room temperature testing,

this version continues to be used at JHU on a daily basis. A newer edition, designed specifically for addressing the challenges associated with processing images taken in a furnace during heating, is in the final stages of development and will also be compiled and released soon. This software, named HighCorr for *High* temperature digital image *Correlation*, provides added performance and functionality specifically for direct thermal expansion measurements and is implemented to produce all of the following results discussed herein.

The main functions of HighCorr include automatically creating a list of filenames to be loaded for the analysis as well as automatically generating a rectangular sampling grid at a resolution determined by the user. Once this is finished, the correlation routine begins to process each of the specified image sets and provides the user with information regarding the current progress along with the estimated time to completion for the entire image batch. Upon conclusion of the image correlation step, which is commonly the most time consuming part of the analysis, the program prompts the user to make a selection from a number of post processing options and automatically generates and saves the desired data and figures.

The correlation engine itself is a proprietary, high precision group of functions that can be acquired by purchasing a current version of Matlab™ with the Image Processing Toolbox installed. Currently, a correlation subset size of 60 x 60 pixels is used and between 1,000 and 1,500 points are applied to compute the thermal displacement, strain, and CTE of the sample. These settings allow the raw correlation results to possess good resolution without requiring an immense amount of time to complete the job. For a modern AMD-based dual core desktop computer, analysis times on the order of 60 to 90 seconds per image are typical. The raw output of the program, i.e. the material coordinates of each correlation point for a given image, are the arrays X and Y. The number of columns in X and Y is equivalent to the number of images that HighCorr processed while the number of rows in X and Y gives the number of points used for the analysis. Equations 3 and 4 exemplify how the x- and y-components of displacement, u and v, are efficiently calculated by subtracting the initial point position arrays X₀ and Y₀ from X and Y. As for each processing step, HighCorr automatically saves the u and v data files in the .txt format so other applications besides Matlab™ can open and analyze these intermediate results files at a later date with ease.

$$u = X - X_0 \quad (3)$$

$$v = Y - Y_0 \quad (4)$$

Figure 3 illustrates the x-component of the displacement field which corresponds to heating a Rene N5 superalloy specimen from room temperature to 1050 °C. This plot shows that the right side of the sample (pixel locations near 3,000) remained mostly fixed with respect to the camera's reference frame while the left side of the specimen expanded to the left due to the temperature increase. The linearity of the surface in Figure 3 verifies that the sample being testing is indeed homogenous in composition and further confirms that there are no major temperature gradients across its length. When a least squares routine is used to fit a plane to these points, which effectively averages over the y-component of the data, the resulting slope yields the x-component of thermal strain associated with increasing the temperature over the range of 25 °C to 1050 °C. If this same procedure is repeated for each of the intermediate images captured between the start and end temperatures of the test, the thermal strain of the specimen can be quantified as a function of temperature. An example of this for a Rene N5 thermal expansion test utilizing 23 images is provided in Figure 4.

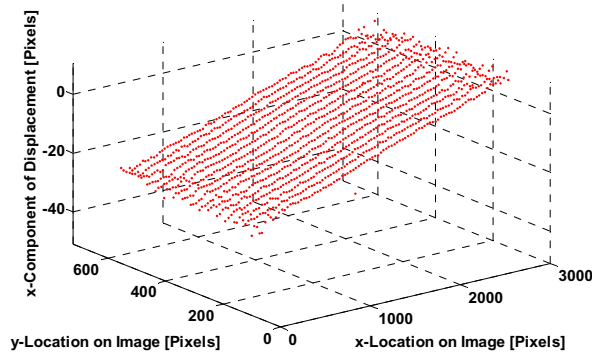


Figure 3. Correlated displacement field at 1050 °C for Rene N5.

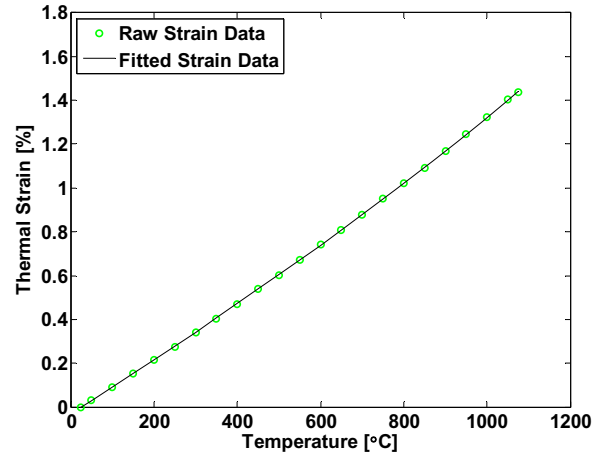


Figure 4. Raw and fitted thermal strain results for Rene N5.

In order to determine the rate of change of thermal strain with respect to temperature, and therefore the CTE for the test, a low order least squares polynomial fit (generally of order four) is applied to the raw strain data, as shown in Figure 4. Once this is accomplished, the derivative of the fit can then be calculated analytically as specified by Equation 5, yielding the temperature-dependent true coefficient of linear thermal expansion. This final step does an excellent job of reducing the undesired effects that any residual, very small amounts of noise have and allows for smooth CTE vs. temperature curves to be created.

$$\alpha(T) = \frac{d\varepsilon_{xx}}{dT} = \frac{d}{dT} \left(\frac{\partial u}{\partial x} \right) \quad (5)$$

Thus, the experimental and image analysis procedures employed in this work are designed to be straightforward, effective, and robust. The availability of a graphical user interface (GUI) where multiple options can be selected during the pre processing, correlation, and post processing steps, along with the ability to analyze color or grayscale images of multiple formats and samples of many sizes, makes HighCorr an outstanding tool for high temperature contact free thermal expansion experiments. The fast, high precision correlation routine allows for reliable results to be generated from sample surfaces with low contrast; further, large image files with many analysis points do not take long to correlate and usually produce displacement and strain values of very good resolution. Finally, the popular nature of the Matlab™ programming environment makes the HighCorr software easily adjustable to all sorts of other high temperature physical and mechanical property measurements.

RESULTS AND DISCUSSION

The results from four image-based thermal expansion tests conducted on Rene N5 are illustrated in Figure 5, as well as the values gathered by other researchers [26, 27] using a standard push rod dilatometer. The superb agreement between the DIC-based and standard dilatometer figures proves that this technique can effectively capture small changes in CTE, even at very high temperatures, in a noncontacting manner. Figure 6 shows the thermal expansion behavior for a 150 μm thick NiCoCrAlY bond coat. This outcome is also found to be in strong accord with CTE information obtained from push rod dilatometer testing of a bulk NiCoCrAlY alloy of similar composition [27].

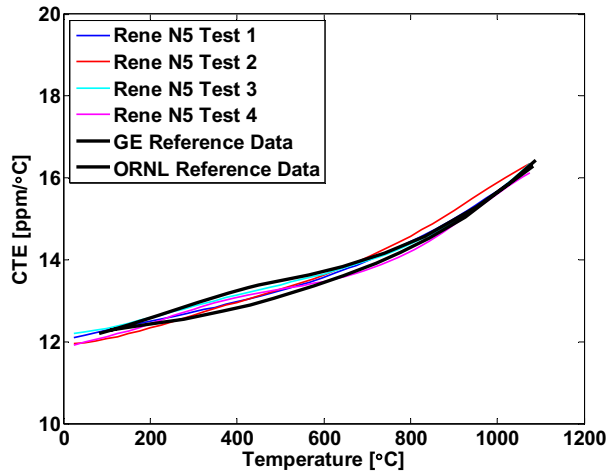


Figure 5. Measured and reference CTE results for Rene N5.

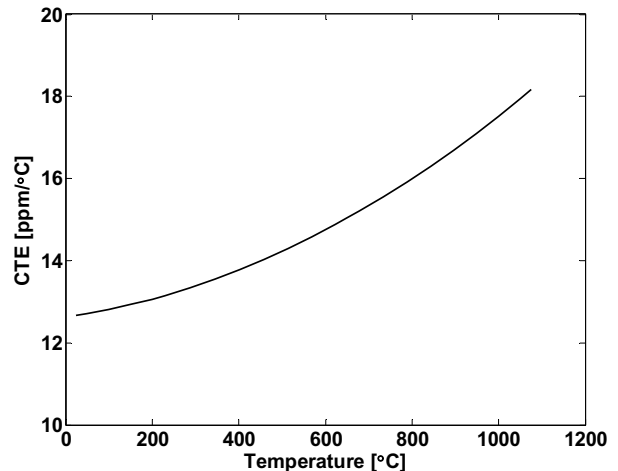


Figure 6. Measured CTE results for a 150 μm thick NiCoCrAlY bond coat.

As a result of bond coat alloys being assumed to be relatively stress free at elevated temperatures, due to both the deposition (formation) temperature as well as the notion that stress relaxation occurs during the high temperature exposures found in service, the values from the tests provided in Figures 5 and 6 suggest that the bond coat desires to contract considerably more than the superalloy substrate upon cooling. This subsequently causes a state of substantial tensile stress to develop in the bond coat. Although NiCoCrAlY bond coat systems are used in current commercial TBC applications, little to no modeling is available. With the data presented above, the magnitude of the mismatch stress, along with its affect on the ultimate failure of the coating, can now begin to be better quantified and understood.

CONCLUDING REMARKS

This paper presents a completely noncontact, robust, easy to use technique for measuring displacement, strain, and the coefficient of thermal expansion of thin specimens at elevated temperatures. The most significant aspects of this study involve the construction and development of a modern experimental setup and novel image correlation tool that allow for precise, temperature-dependent evaluation of CTE to nearly 1100 °C. High costs and complexities are not associated with these abilities, however, as the setup is undemanding to operate and can be built in its entirety for about \$8,000. The flexible nature of the optics and HighCorr software enable the examination of numerous other types of samples that can be unconventional in both shape and size. Direct measurements on Rene N5 and a NiCoCrAlY bond coat elucidate a considerable thermal expansion mismatch that needs to be addressed in more detail in the future. Potential improvements to the current setup include higher quality telecentric optics and a vacuum environment, both of which would increase costs substantially but also allow for the accurate testing of extremely thin specimens where oxide formation is more important and undesirable. Nonetheless, the overall effectiveness of the existing experimental and image processing procedure are sufficient for the current alloys and geometries that require assessment; many more high temperature thermal expansion tests are planned for the near future.

ACKNOWLEDGEMENTS

The authors would like to acknowledge the National Science Foundation Division of Materials Research for supporting this work (Grant No. DMR-0413803). Prof. W. Sharpe Jr., Dr. C. Eberl, and Dr. D. Gianola provided many useful suggestions during the setup development and testing

phase of the project; their assistance is greatly appreciated as well. Lastly, thanks go out to Dr. R. Darolia at GE and Dr. M. Maloney at Pratt and Whitney for supplying the alloys used for the thermal expansion experiments.

REFERENCES

1. Evans A., Mumm D., Hutchinson J., Meier G., and Pettit F., Mechanisms controlling the durability of thermal barrier coatings, *Progress in Materials Science*, 46: 505-553, 2001.
2. Ambrico J., Begley M., and Jordan E., Stress and shape evolution of irregularities in oxide films on elastic-plastic substrates due to thermal cycling and film growth, *Acta Materialia*, 49: 1577-1588, 2001.
3. Balint D. and Hutchinson J., An analytical model of rumpling in thermal barrier coatings, *Journal of the Mechanics and Physics of Solids*, 53: 949-973, 2005.
4. Touloukian Y., Kirby R., Taylor R., and Desai P., eds., *Thermophysical Properties of Matter - the TPRC Data Series, Volume 12: Thermal Expansion - Metallic Elements and Alloys*, Plenum, 1975.
5. James J., Spittle J., Brown S., and Evans R., A review of measurement techniques for the thermal expansion coefficient of metals and alloys at elevated temperatures, *Measurement Science and Technology*, 12: 1-15, 2001.
6. Knibbs R., The measurement of thermal expansion coefficient of tungsten at elevated temperatures, *Journal of Physics E Scientific Instruments*, 2: 515-517, 1969.
7. Riess I., Electro-optical dilatometer, *Journal of Physics E Scientific Instruments*, 20: 257-259, 1987.
8. Raether F., Springer R., and Beyer S., Optical dilatometry for the control of microstructure development during sintering, *Materials Research Innovations*, 4: 245-250, 2001.
9. Paganelli M., Using the optical dilatometer: To determine sintering behavior, *American Ceramic Society Bulletin*, 81: 25-30, 2002.
10. Bennett S., An absolute interferometric dilatometer, *Journal of Physics E Scientific Instruments*, 10: 525-530, 1977.
11. Okaji M. and Imai H., A high-temperature dilatometer using optical heterodyne interferometry, *Journal of Physics E Scientific Instruments*, 20: 887-891, 1987.
12. Wantanabe H., Yamada N., and Okaji M., Development of a laser interferometric dilatometer for measurements of thermal expansion of solids in the temperature range 300 to 1300 K, *International Journal of Thermophysics*, 23: 543-554, 2002.
13. Peters W. and Ranson W., Digital imaging techniques in experimental stress analysis, *Optical Engineering*, 21: 427-431, 1982.
14. Chu T., Ranson W., Sutton M., and Peters W., Applications of digital image correlation techniques to experimental mechanics, *Experimental Mechanics*, 25: 232-244, 1985.
15. Sutton M., Wolters W., Peters W., Ranson W., and McNeill S., Determination of displacements using an improved digital correlation method, *Image and Vision Computing*, 1: 133-139, 1983.

16. Sutton M., Cheng M., Peters W., Chao Y., and McNeill S., Application of an optimized digital correlation method to planar deformation analysis, *Image and Vision Computing*, 4: 143-150, 1986.
17. Bruck H., McNeill S., Sutton M., and Peters W., Digital image correlation using newton-raphson method of partial differential correction, *Experimental Mechanics*, 29: 261-267, 1989.
18. Vendroux G. and Knauss W., Submicron deformation field measurements: Part 2. Improved digital image correlation, *Experimental Mechanics*, 38: 86-92, 1998.
19. Coburn D. and Slevin J., Digital correlation system for nondestructive testing of thermally stressed ceramics, *Applied Optics*, 34: 5977-5986, 1995.
20. Lyons J., Liu J., and Sutton M., High-temperature deformation measurements using digital image correlation, *Experimental Mechanics*, 36: 64-70, 1996.
21. Anwander M., Zagar B., Weiss B., and Weiss H., Noncontacting strain measurements at high temperatures by the digital laser speckle technique, *Experimental Mechanics*, 40: 98-105, 2000.
22. Volkl R. and Fischer B., Mechanical testing of ultra-high temperature alloys, *Experimental Mechanics*, 44: 121-127, 2004.
23. Beghini M., Bertini L., and Frenzo F., Thermal expansion coefficient of a NiCoCrAlY-ZrO₂(Y₂O₃) coating by a digital image processing based dilatometer, *International Journal of Materials and Product Technology*, 15: 78-90, 2000.
24. Eberl C., Thompson R., Gianola D., Sharpe Jr. W., and Hemker K., *Digital image correlation and tracking*, <http://www.mathworks.com/matlabcentral/fileexchange>, 2006.
25. Sharpe Jr. W., Pulskamp J., Gianola D., Eberl C., Polcawich R., and Thompson R., Strain measurements of silicon dioxide microspecimens by digital image processing, *Proceedings of the SEM Annual Conference and Exposition on Experimental and Applied Mechanics*, 2: 1056-1061, 2006.
26. Darolia R., Private communications, 2006.
27. Haynes J., Pint B., Porter W., and Wright I., Comparison of thermal expansion and oxidation behavior of various high-temperature coating materials and superalloys, *Materials at High Temperatures*, 21: 87-94, 2004.